NiMo/MCM-41 Catalysts for the Hydrotreatment of Polychlorinated Biphenyls

Franklin J. Méndez · Ernesto Bastardo-González · Paulino Betancourt · Luis Paiva · Joaquín L. Brito

Abstract MCM-41 type mesoporous materials of pure silicon and aluminosilicates (with Si/Al atomic ratios of 20 and 40) were prepared by a facile synthesis method and used to support NiMo catalysts. Characterization by XRD showed typical patterns of this type of mesoporous solids with a partial collapse of the structure on increasing Al content. In addition, signals attributed to the formation of MoO_3, NiO and $Al_2(MoO_4)_3$ in the transition-metal containing catalysts were observed. The ^{29}Si-NMR-MAS spectra showed that local arrangement of the Si–O–Si bonds was regular, independently of the solid being pure or modified with Al, while the ^{27}Al-MAS-NMR spectra of the aluminosilicates showed both structural and non-reticular species. The N_2 adsorption–desorption curves showed type IV isotherms, with considerable diminution in the BET areas once the metals were incorporated. The catalytic results in thiophene hydrodesulfurization (HDS) and polychlorinated biphenyl hydrodechlorination (HDCl) revealed a considerable catalytic activity for all prepared catalysts as compared with a commercial $NiMo/Al_2O_3$ one, being highest in the case of the NiMo/Al-MCM-41(40) one for HDS, and for NiMo/Al-MCM-41(20) in HDCl. The excellent properties for HDCl can be attributed to good dispersion of Ni and Mo active phases and to the bifunctional character of the catalysts, namely, to the participation of both coordinatively unsaturated sites of the NiMoS active phase and Brønsted acid sites of the support.

Keywords Hydrodechlorination · Hydrodesulfurization · MCM-41 synthesis · NiMo · Sulfided catalysts

F. J. Méndez · P. Betancourt (✉) · J. L. Brito (✉)
Laboratorio de Fisicoquímica de Superfícies, Centro de Química, Instituto Venezolano de Investigaciones Científicas, Apartado 20632, Caracas 1020, Venezuela
e-mail: paulino.betancourt@gmail.com

J. L. Brito
e-mail: joabrito@ivic.gob.ve

E. Bastardo-González (✉)
Laboratorio de Química de Superfícies, Departamento de Química, Universidad de Oriente, Cumaná, Venezuela
e-mail: ernieluis@hotmail.com

P. Betancourt · L. Paiva
Laboratorio de Tratamiento Catalítico de Efluentes, Centro de Catálisis, Petróleo y Petroquímica, Universidad Central de Venezuela, Caracas, Venezuela

1 Introduction

Considerable effort is aimed nowadays at improving hydrotreatment (HDT) catalysts, especially for the hydrodesulfurization (HDS) reaction [1]. From an environmental point of view, the main purpose of removing sulfur from petroleum and its derivatives is to reduce the sulfur dioxide emissions that result from using fossil fuel. Another important reason is that sulfur, even in low concentrations, poisons the noble metal catalysts in the catalytic reforming units that are used subsequently to HDT in order to upgrade the octane rating of the naphtha streams [1, 2]. Finally, sulfur compounds have a deleterious, corroding effect on refinery equipment.

Polychlorinated biphenyls (PCBs), on the other hand, are considered priority pollutants [3] due to their widespread presence in the environment and tendency to increasingly accumulate in the fatty tissues of living beings along the chain food up to humans. The disposal of PCBs is principally carried out by high-temperature incineration. However, this method may promote the formation of even more toxic polychlorinated dibenzofurans and polychlorinated dibenzodioxins [4].

Therefore, much research has been conducted on non-thermal oxidation methods of degrading PCBs with simultaneous recovery of the hydrocarbons formed and their recycling as valuable products [5]. The catalytic hydrodechlorination (HDCl) is a potential technology to carry out complete removal of such persistent pollutants.

Noble and transition metal catalysts loaded on alumina, silica and carbon have been usually employed for HDCl reactions. The dechlorination of organic chlorinated compounds using supported Pd, Pt, Rh and Ni has been widely reported [6–16]. A few studies on the HDCl process of PCBs were carried out using commercial-like hydroprocessing catalysts, mainly $NiMo/Al_2O_3$ and $CoMo/Al_2O_3$ [17–22]. These catalysts were found to be more resistant to deactivation by HCl formed as compared to noble metal based catalysts, operating, however, under more severe conditions (250–350 °C, high pressure of hydrogen). NiMo catalysts can be used in their oxidic (reduced) or sulfided forms, although it was reported that the sulfided NiMo/ Al_2O_3 catalyst shows a higher activity [23]. Compared to the catalytic processes, the thermal hydrogenolysis of chloroarenes, including PCBs, in hydrogen atmosphere requires much higher temperatures, in the range of 700–925 °C [24].

The need to improve the efficiency of industrial catalysts in several processes has prompted the study and development of new formulations, based on support modification that can provide a suitable porous structure [25]. Research has shown that the proper choice of support is of great importance for the enhancement of catalytic HDT in general and to work under less severe reaction conditions in particular. Mesoporous molecular sieves, with pores of 20–35 Å in diameter, surface areas of 700–1,000 $m^2 g^{-1}$ and intermediate acidity, have attracted much interest for petroleum HDT processes [1, 26–28]. The silica based M41S materials, discovered in the early 1990s [29], are a very interesting class of mesoporous materials. The Si-MCM-41, which has a hexagonally-ordered pore structure, is the most stable and important phase in the M41S family. As is the case with other zeotypes, it is possible to partially substitute Al^{3+} for Si^{4+} ions (herein designated both as (Si/Al)-MCM-41-(X) and Al-MCM-41-(X), where X stands for the atomic Si/Al ratio). The hexagonal mesoporous system with high surface area opens possibilities for accepting the impurities with high kinetic diameters contained in the oil fractions, as well as other large molecules such as PCBs. Indeed, conventional supports employed for HDT catalysts, usually consisting mainly of γ-alumina, possess an important fraction of mesopores as part of bimodal porous systems [1]. However, it can be expected that a more ordered structure such as that of M41S solids provides larger surface areas and easier acces to the internal porous structure. The formation of Si-MCM-41 and (Si/Al)-MCM-41 phases occurs according to the liquid crystal template mechanism, in which SiO_4 and AlO_4 tetrahedra react with the surfactant template under hydrothermal conditions, generally involving the use of an autoclave and/or long aging times at high temperatures.

Several works have been published concerning NiMo catalysts supported on Si-MCM-41 and (Si/Al)-MCM-41 for thiophene and dibenzothiophene HDS reactions [30–35]. These catalysts have shown good catalytic properties during HDS when they are compared with the conventional catalysts. To our best knowledge, however, no study has been done by using NiMo or CoMo catalysts supported on MCM-41 supports for HDCl reactions. Instead, a few works have been reported on the use of monometalic catalysts based on Ni, Pd and Pt on mesoporous MCM-41-type materials. Thus, Ni/Al-MCM-41 was tested in gas phase HDCl of 1,2,4-trichlorobenzene, showing high activity and selectivity towards benzene at reaction temperatures between 473 and 523 K with values of 100 % conversion and 100 % selectivity at 523 K [36]. Subsequently, Pd/Si-MCM-41 catalyst showed high activity for the hydrodehalogenation of aryl halides [37]. Furthermore, supported Pd catalysts prepared by the template-ion exchange method on Al-substituted MCM-41 presented high activity in the HDCl of aryl chlorides substituted by hydroxyl, methoxy, methyl, nitro and phenylcarbonyl group at the *p*-position. These compounds were efficiently dechlorinated in the presence of triethylamine over Pd/Al-MCM-41 catalyst [38]. More recently, Pt/Si-MCM-41 and Pd/Si-MCM-41 were tested in the HDCl of 1,2-dichloroethane. The improvement of activity was related to the higher surface area of the support, as well as to the higher concentration of (–OH) terminal groups, which induced a better dispersion of the metal particles [39].

It is reported in this work an easy method of synthesis of (Si/Al)-MCM-41 mesoporous materials and their performance as supports of NiMo phases in the HDT of thiophene and polychlorinated biphenyls. Due to the versatility and efficiency of $NiMo/Al_2O_3$ catalysts in the HDS and HDCl reactions, coupled with exceptional properties shown by the Ni, Pd and Pt catalysts supported on Si-MCM-41 and (Si/Al)-MCM-41 for HDCl, it is expected that the NiMo/(Si/Al)-MCM-41 formulations might also show excellent catalytic behavior in both these HDT reactions.

2 Experimental

2.1 Synthesis of Si-MCM-41

$NaOH/SiO_2$ solution (SOL-I) was prepared with 400 mol of NaOH (Riedel-de Haën) in 80 mL of deionized water followed by addition of 200 mol of SiO_2 (Sigma-Aldrich). The initial suspension was maintained under magnetic stirring at

~70 °C until obtaining a homogeneous solution. Afterwards, magnetic stirring was kept while cooling down until reaching room temperature. In parallel, a surfactant solution (SOL-II) was prepared, homogenizing 48.0 mol of tetramethylammonium hydroxide (TMAOH, Sigma-Aldrich) in 150 mL of deionized water followed by addition of 50.0 mmol of cetyltrimethylammonium bromide (CTMABr, Sigma-Aldrich), until complete dispersion. Subsequently, SOL-I was added to SOL-II, pH was adjusted to ~9.0 with H_2SO_4 (Fluka), keeping under magnetic agitation for 2 h. The resulting mixture was aged for 24 h. The gel formed was vacuum-filtered and the resulting solid was dried, pulverized and calcined at 550 °C for 8 h.

2.2 Synthesis of (Si/Al)-MCM-41(X) (X = Si/Al Atomic Ratio)

SOL-III was prepared by dispersing aluminum isopropoxide (Sigma-Aldrich) in 35.0 mL of isopropanol (Sigma-Aldrich) and heating by means of a glycerol bath (Fluka) at ~70 °C. On the other hand, 46.0 mL of tetraethylorthosilicate (TEOS, Sigma-Aldrich) was added to 80.0 mL of absolute ethanol (Riedel-de Haën) (SOL-IV). This solution was added to SOL-III, previously cooled to room temperature. The resulting suspension (SOL-V) was placed in a glycerol bath, under magnetic stirring at ~70 °C for 4 h. Simultaneously, it was prepared a surfactant solution (SOL-II) and added to SOL-V. The gel formed was treated in the same way as above (pH adjustment, aging, drying and calcining), obtaining the aluminosilicates with Si/Al atomic ratio X = 40 and 20.

2.3 Supported Bimetallic Catalyst Preparation

Ni and Mo species, in atomic ratio 1:3, were deposited on either support by the successive incipient impregnation method. First, the support was impregnated with an appropriate amount of $Ni(NO_3)_2 \bullet 6H_2O$ (Riedel-de Haën) in aqueous solution, dried (60 °C/2 h) and calcined (500 °C/4 h). Subsequently, the Ni-containing sample was impregnated in same way with $(NH_4)_6Mo_7O_{24} \cdot 4H_2O$ (Riedel-de Haën), and then dried and calcined under the same conditions, thus obtaining the supported NiMo catalysts.

2.4 Physicochemical Characterization

Powder X-ray diffraction (XRD) was carried out with a Phillips PW710 diffractometer using Cu-Kα radiation ($\lambda = 1.5456$ Å) and Ni filter. The small-angle XRD pattern was scanned between 0.5° and 10°, while wide-angle XRD measurements was set between 20° and 50°, both with a step rate of 0.02°/s. The identification of the different phases was made using the JCPDS library [40].

Solid state magic angle spinning-nuclear magnetic resonance (^{29}Si and ^{27}Al-MAS-NMR), was carried out using a Bruker ADVANCE 300. The spectra were recorded at 25 °C, at a source frequency of 59.63 MHz (^{29}Si) and 78.219 MHz (^{27}Al).

Nitrogen adsorption/desorption isotherms were measured with a Micromeritics-ASAP 2010 automatic analyzer at liquid N_2 temperature. Prior to the experiments, the samples were degassed overnight under vacuum at 60 °C. Specific surface areas were calculated by the Brunauer-Emmett-Teller method (S_{BET}), the pore volume (V_p) was determined by N_2 adsorption at a relative pressure of 0.98 and pore size distributions from the desorption isotherms by means of the Barret-Joyner-Halenda (BJH) method.

2.5 Catalytic Activity Measurements

2.5.1 Thiophene Hydrodesulfurization

Catalyst samples (300 mg) were activated in situ in a 100 mL/min flow of a CS_2/H_2 mixture (1 vol% CS_2) for 2 h at 300 °C. Tests of thiophene HDS were carried out as reported elsewhere [41] at 400 °C and atmospheric pressure under a 100 mL/min flow of a thiophene/H_2 mixture (2.27 mol% thiophene). Reaction products were analyzed by means of FID gas chromatography, with sampling of the gas effluent occurring typically at 8 min intervals.

2.5.2 Polychlorinated Biphenyl Hydrodechlorination

The experimental reaction system was designed to work under high pressure. A fixed-bed flow reactor (stainless-steel tube with an internal diameter of 16 mm) was packed with 300 mg of catalyst particles. The catalyst was presulfided using a mixture of 2 vol% H_2S in H_2 at 300 °C for 1 h. After presulfidation, the reactor was cooled down in the H_2S/H_2 stream to the desired temperature and thereafter it was pressurized with hydrogen. The reactant solution (PCBs in heptane) was then introduced into the reactor by means of a high-pressure liquid pump (Isco 65D). The PCB HDCl reaction was carried out under the following conditions: temperature 350 °C; total pressure 3.5 MPa; WHSV 28 h; flow rate of liquid 32 mL/h; flow rate of H_2 25 L/h; initial concentration of PCBs 0.05–1.0 wt%; H_2S partial pressure 0.3×10^5 Pa. Aroclor® 1242 was a sample taken from laboratory stock (kindly supplied by PDVSA-Intevep).

After steady state was reached (about 2 h), three samples of liquid products were collected from a gas–liquid separator every 30 min. The activity was taken as the mean value obtained for three samples. For each set of experiments a back point was taken to check if any deactivation occurred. The collected samples were analyzed by GC–MS with a HP 5973 mass detector coupled to an HP 6890 GC, equipped

with an HP-5MS capillary column of 30 m × 0.25 mm, film thickness 0.25 μm. The oven temperature program was an initial hold for 1 min at 50 °C, followed by a ramp at 10 °C/min, to 300 °C and another hold for a further 3 min prior to cooling down. Calibration was performed by the method of external standards and as the final stage of sample preparation; hexadecane was added to all samples as an internal standard.

It must be stressed that the analysis on PCBs is rather difficult due to accuracy problems in PCBs detection which are attributed to deterioration in sensitivity and background induced by interfering components in analytical media. However, we employed an accepted standard method (ASTM D4059) [42]. The presence of HCl was detected both in the gas phase and on the catalyst after extraction with alkaline solutions. However, the amount of HCl measured generally did not satisfy the mass balance. In this work the effect of the produced HCl on HDCl was not studied.

3 Results and Discussion

The synthesis method described in this work allowed to obtain solids with M41S structure without employing hydrothermal conditions and using shorter times and lower temperatures than most reported synthesis procedures. Both the uncalcined and the calcined Si-MCM-41 samples were examined by XRD, and the patterns are shown in Fig. 1. It can be seen that, before calcination, this solid exhibits an intense reflection at $2\theta = 2.84°$ and three weaker ones at 4.36°, 4.92° and 6.26° assigned respectively to the (100) (110) (200) and (210) characteristic reflections of Si-MCM-41. The calcined sample shows the reflections mentioned above with a greater definition and sharpness, indicating that the Si-MCM-41 mesostructure is retained after calcination [29]. Additionally, upon calcination it can be seen the shift of these reflections toward higher 2θ values, indicating a contraction of the structure, due to the removal of the organic part of the micelles and condensation of silanol groups (Si–OH), resulting in a more compact structure with higher structural order. This produces a larger amount of fully condensed Si atoms, $Si(OSi)_4$ [29, 43].

Several authors have reported that the incorporation of cationic elements, such as aluminum, in Si-MCM-41 produces significant changes in the structure and properties of the resulting materials [25, 44, 45]. Figure 2 shows the decrease in the relative intensities and partial disappearance of the (110) (200) and (210) reflections and the increased width of the basal reflection with increasing amount of aluminum. These results suggest a deterioration of the hexagonal structure as a result of isomorphic substitution, as well as a decrease in particle size [29, 33, 45–47]. Additionally,
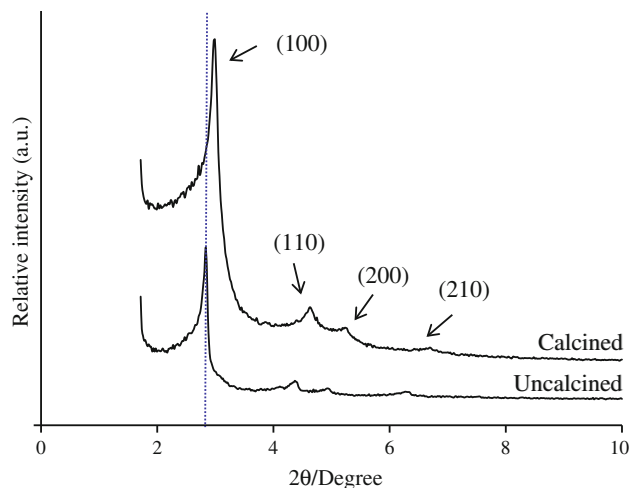

Fig. 1 Small-angle XRD patterns of calcined and uncalcined samples of Si-MCM-41

the basal reflection shifts towards lower values of 2θ, indicating the incorporation of aluminum, which results in an expansion of the structure. These results were confirmed by the increased wall thickness (δ), lattice parameters (a_o) and interplanar distance (d_{100}), as can be seen in Table 1.

Figure 3 shows the XRD patterns of calcined catalysts. It can be noticed an intense reflection at 27.30° and six weaker ones at 23.34°, 25.68°, 28.72°, 33.72°, 38.88° and 49.24°, assigned to orthorhombic MoO_3 (JCPDS card 5-0506) [40]. Furthermore, a smaller reflection at 2θ of 43.22° is assigned to NiO in the hexagonal phase (JCPDS card 44-1159) [40]. The intensities of the peaks located at 23.34° and 25.68°, especially the latter one, increase with Al loading, suggesting the formation of $Al_2(MoO_4)_3$ (JCPDS card 23-0764) [33, 40], confirmed by a peak located at 26.22° and two smaller reflections at 23.22° and
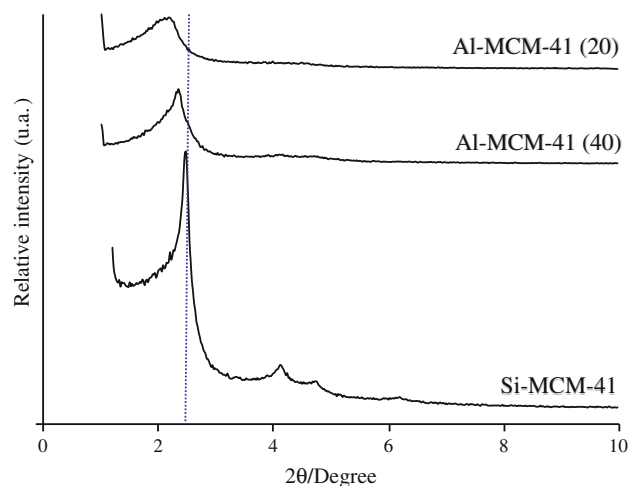

Fig. 2 Small-angle XRD patterns of the calcined (Si/Al)-MCM-41 supports

Table 1 Textural and structural characteristics of solids

Sample	d_{100} (Å)	a_0 (Å)[a]	S_{BET} (m^2/g)	V_p (cm^3/g)	D_p (Å)[b]	δ (Å)[c]
Si-MCM-41	35.3	40.8	1,124	0.88	30	11
Al-MCM-41(40)	36.6	42.3	898	0.87	30	12
Al-MCM-41(20)	39.0	45.0	784	0.65	27	18
NiMo/Si-MCM-41	–	–	763	0.68	28	–
NiMo/Al-MCM-41(40)	–	–	678	0.67	30	–
NiMo/Al-MCM-41(20)	–	–	609	0.58	25	–

[a] Lattice parameter (a_0) for a hexagonal structure: $a_0 = 2d_{100}/\sqrt{3}$

[b] Pore diameter (D_p) determined from the desorption isotherms by the BJH method

[c] Pore wall thickness (δ) estimated by $\delta = a_0 - D_p$

23.50°. This mixed phase is probably formed at the expense of extra-reticular Al species (see below).

Solid-state ^{29}Si-MAS-NMR and ^{27}Al-MAS-NMR spectra are shown in Figs. 4 and 5, respectively. Figure 4 shows similar spectra for the different solids, indicating that the local arrangement of the Si–O–Si bonds at the pore walls is regular and that the angle between these bonds varies over an ample range. This figure also shows that similarly to amorphous silica, part of the Si atoms exist as silanol groups. The resonance peaks at −112.14, −102.72 and −92.02 ppm have been attributed to the Si(OSi)$_4$, Si(OSi)$_3$OH and Si(OSi)$_2$(OH)$_2$ environments, generally labeled as Q$_4$ (framework), Q$_3$ (silanol) and Q$_2$ (disilanol), respectively. The presence of Al atoms in the network may generate Si(3Si,Al) and Si(2Si,2Al) environments, which might be contributing to the resonance peak intensities at −102.72 and −92.02 ppm [48]. On the other hand, the ^{27}Al-MAS-NMR spectra of the calcined (Si/Al)-MCM-41(X) samples (Fig. 5), present a resonance peak at 53.79 ppm which is attributed to structural tetrahedrally coordinated aluminum. Furthermore, a peak around 0 ppm is representative of hexacoordinated aluminum belonging to extra-structural species formed during calcination [48, 49].

The Si-MCM-41 sample presented a bimodal adsorption isotherm characteristic of well-formed M41S materials (Fig. 6) with micro- and mesoporosity, and showing the highest surface area and the smallest pore wall thickness among these samples (Table 1). Incorporation of Al during the synthesis produces a drop in surface area and total pore volume that is more significant at higher Al content (X = 20). The shape of the adsorption isotherms of the aluminosilicates is similar to that of Si-MCM-41. However, as the Al loading increases, the adsorption at low relative pressure (p/p^0 between 0.2 and 0.3), characteristically high for Si-MCM-41, becomes substantially smaller indicating less microporosity and a relatively broad pore size distribution [48].
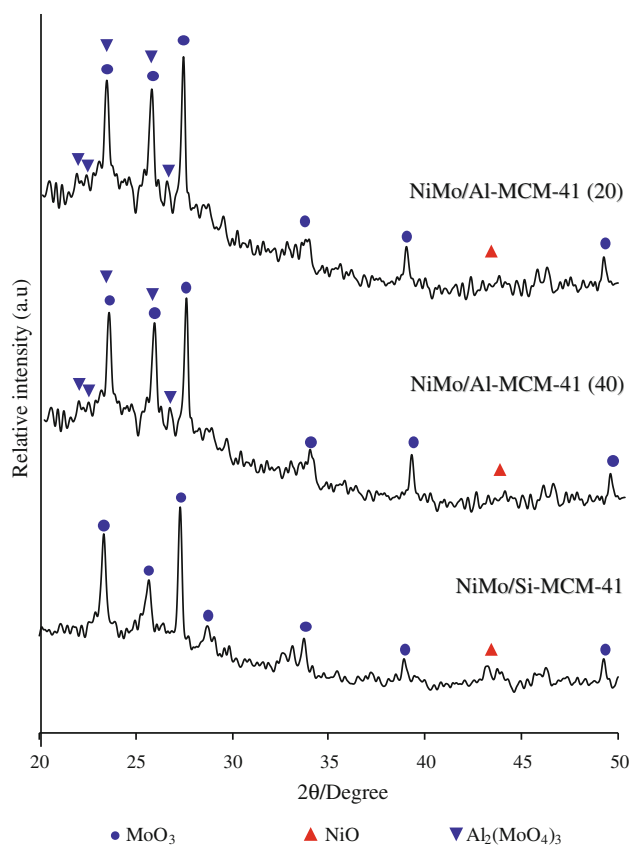

Fig. 3 XRD patterns of calcined, MCM-41 supported NiMo catalysts

The increment of the pore wall thickness is an evidence of the isomorphous substitution of the larger Al^{3+} for Si^{4+} ions (Table 1). However, the decrement in surface area and pore volume together with the small-angle XRD observations that show a decrease in the intensity of the (100) reflection and its broadening, following incorporation of Al atoms (Fig. 2), indicate that the local structure of aluminosilicate is less uniform than that of the purely siliceous material [50]. This suggests partial destruction of the pore arrangement and possibly the existence of some amorphous domains in the (Si/Al)-MCM-41 samples.

A significant decrease in surface area and pore volume is observed when Ni and Mo oxides are incorporated to the supports (Table 1). This decrease is more pronounced for the catalysts supported on the pure siliceous material, which could be due to pore blockage caused by a low dispersion of the metal phases (Mo and Ni), in agreement with earlier published data that evidenced the low dispersion of molybdate in SiO$_2$-supported catalysts [51, 52].

The catalytic performance of supported NiMo catalysts was first evaluated through the HDS of thiophene. Figure 7 shows the thiophene conversion percent as a function of reaction time. In all cases, high initial values of conversion were obtained which decreased progressively and reached a steady state value after more than 60 min of reaction
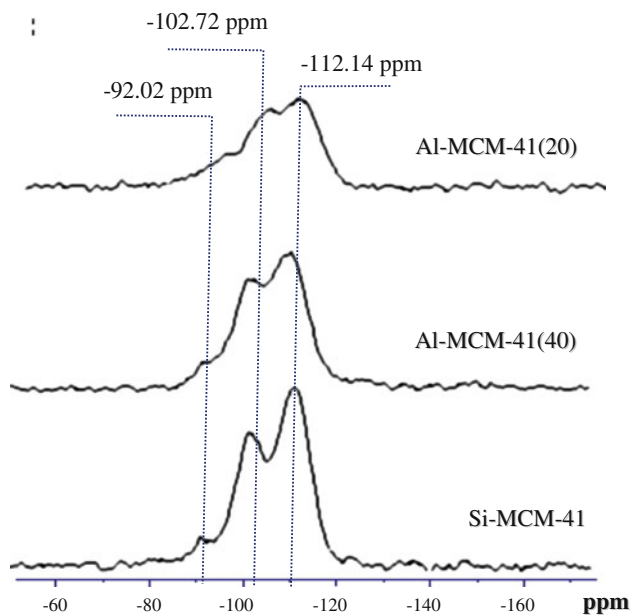
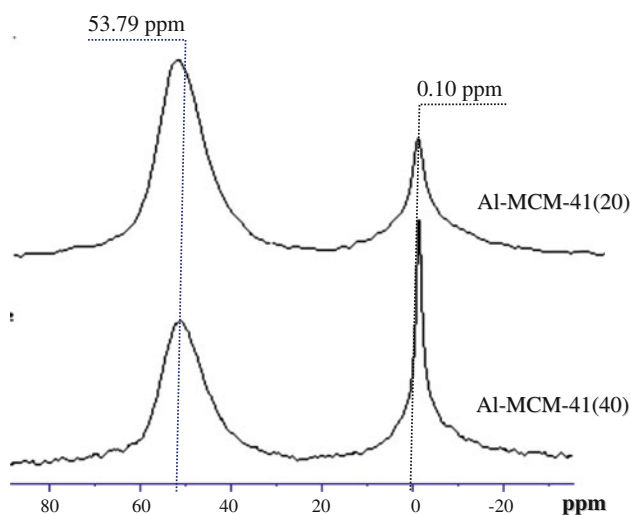Fig. 4 Solid-state ^{29}Si-MAS-NMR spectra of the mesoporous supports

Fig. 5 Solid-state ^{27}Al-MAS-NMR spectra of aluminosilicate supports

Fig. 6 Nitrogen adsorption–desorption isotherms of mesoporous supports

time. Taking in consideration the conversion values obtained at 180 min, the following order was observed: NiMo/(Si/Al)-MCM-41(40) > NiMo/(Si/Al)-MCM-41(20) > NiMo/Si-MCM-41. Similar results, as regards to M-41S type support composition, have been observed previously [31, 33]. In the case of NiMo/Al$_2$O$_3$ commercial sample, the conversion at 180 min was similar to that of the NiMo/(Si/Al)-MCM-41(20) sample, although the extent of deactivation was lower.

The HDS activity trend with the composition change of the Al-containing MCM-41 supports would be the result of
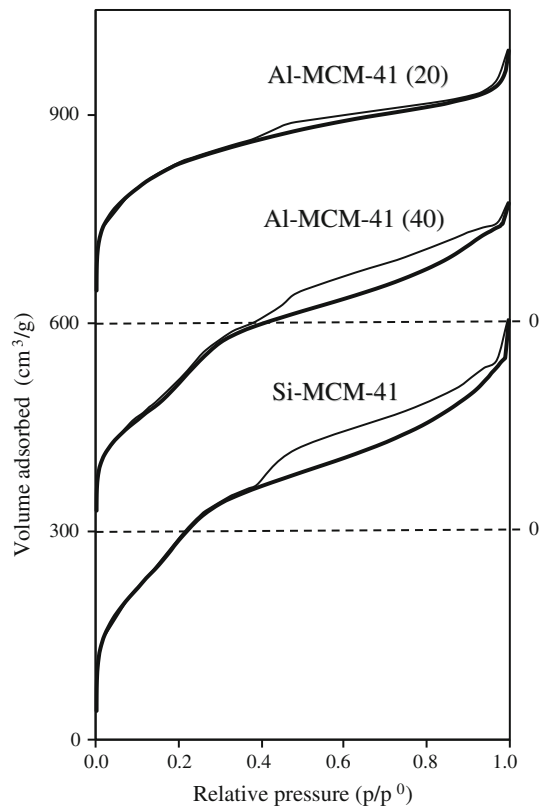
two opposite effects: On one hand, the incorporation of aluminum onto the mesoporous support surface provides a larger number of hydroxyl groups as compared to the support with only silicon, allowing a better dispersion of the molybdenum and nickel oxidic and sulfided phases [31, 33]. This is the result of formation of a high number of stronger Bronsted acid sites in the mixed support as compared with those of pure silica. On the other hand, too strong metal-support interaction inhibits the reduction and sulfidation of Ni and Mo species, processes which are required to generate the active phases, thus resulting in decreased HDS activity. This would be the case of NiMo/(Si/Al)-MCM-41(20) catalyst, due to the presence of stronger acid sites at higher Al contents [33].

The initial deactivation of the catalysts could be ascribed to carbon deposits formation [41] and/or rearrangements of the active sulfided phases during the first stage of reaction. The formation of carbon residua would be more important in the more acidic solids (silico-aluminates) than on the commercial catalyst, as observed in Fig. 7. The strong deactivation of the pure silica supported catalyst could be due to the lower interaction between active phase and support, allowing restructuring of the supported sulfides whose dispersion would be decreased [51, 52].
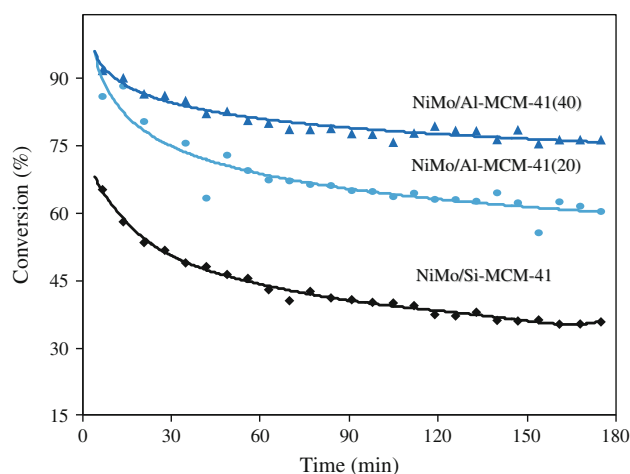
Fig. 7 Thiophene HDS over MCM-41 supported NiMo catalysts

Fig. 8 HDCl of Aroclor® 1242 over MCM-41 supported NiMo catalysts

The catalytic activities of the sulfided MCM-41 supported catalysts were examined in the HDCl of Aroclor® 1242, and compared with the commercial NiMo/Al$_2$O$_3$ catalyst. Figure 8 shows the HDCl conversion in function of time for all the catalyst samples. Similarly to the results for HDS in Fig. 7, the initial activity is higher and decreases with increasing time, however, the activity loss is lower for the HDCl reaction. In Fig. 8 it can be observed that PCBs conversion reached at 2 h varies with support composition in a wide range. Thus, high catalytic activity (49 % of PCBs conversion) is reached for the catalysts supported on (Si/Al)-MCM-41(20). PCBs conversion of NiMo catalyst supported on (Si/Al)-MCM-41(40) is lower and equal to that of the catalyst supported on the pure silica support (34 %). The commercial NiMo/Al$_2$O$_3$ catalyst shows the lowest HDCl conversion (8 %). Elsewhere [18–22] it has been reported that the commercial-like CoMo and NiMo catalysts supported on alumina are very effective catalysts for HDCl of BPCs, hence, the inclusion of MCM-41 type supports has improved significantly the HDCl catalytic properties. This considerable improvement would be the result of a more uniform pore size distribution with larger pore diameters, favoring the diffusion into the porous system of the big PCBs molecules. For the case of the smaller thiophene molecule, employed in this work for the HDS experiments, no such effect is observed but it would be more noticeable if bulkier benzo- and dibenzothiphenes were emploied as feeds.

The HDCl activity trend with the change of the Al content of the MCM-41 support is different than that observed above for HDS. Thus for the highest Al content the maximum HDCl conversion was observed, while the support with lower Al content shows a similar conversion than the siliceous material. This suggests that the NiMoS active phases behave distinctly for either reaction.
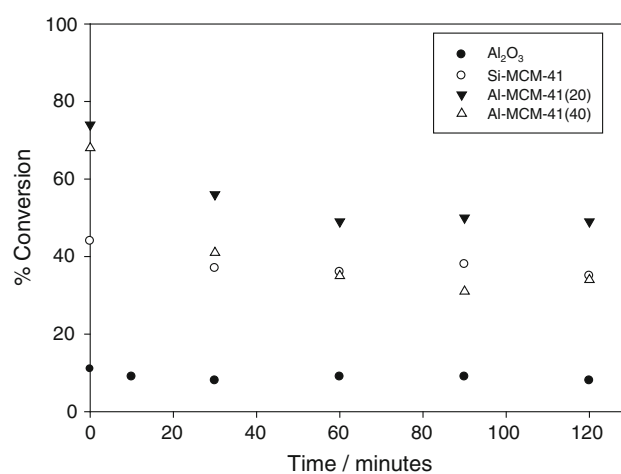
It is known that the HDCl of PCBs occurs through several consecutive reaction steps each of them determining the substitution of a single chlorine atom [6, 18–21]. When Al-atoms are incorporated into the MCM-41-support, the amounts of HDCl products increase, probably because of better dispersion of the MoS$_2$ active phase. Additionally, for the NiMo catalysts supported on (Si/Al)-MCM-41(20) it was observed the preferential formation of the hydrogenated isomers (chlorocyclohexyl-chlorobenzene) of the dichlorinated BPCs (Table 2). This observation points out the bifunctional character of these active catalysts. Both types of sites, coordinatively unsaturated sites (CUS) of the NiMoS active phase and Brønsted acidic protons of the support, participate in the catalytic transformations of PCBs. The Brønsted acid site isomerizes the PCBs changing the position of the chlorine substituent in the molecule. This reduces the steric hindrance of chlorine groups and makes the following dechlorination on CUS more facile. In addition, the better dispersed NiMoS phases in the highest Al content support favour the hydrogenation of the aromatic cycle. Therefore, high catalytic performance of these catalysts in HDCl of PCBs can be attributed to the synergism between both types of active sites.

Table 2 Selectivity to dichlorinated products of HDCl

Sample	% Selectivity	
	CCH-CB	DCBP
NiMo/Si-MCM-41	8.6	0.4
NiMo/Al-MCM-41(20)	14.0	1.5
NiMo/Al-MCM-41(40)	9.1	3.0

CCH-CB chlorocyclohexyl-chlorobenzene, *DCBP* dichlorobiphenyl

4 Conclusions

A facile synthesis method for MCM-41 materials, which does not involve hydrothermal treatments, has been employed to synthesize both siliceous and silico-aluminous supports for HDT catalysts. It has been found that varying Si/Al ratios lead to different reactivities in HDS and HDCl, likely as result of distinct characteristics of the active phases on the supports. Thus, the NiMo/(Si/Al)-MCM-41(40) material showed the highest conversion levels of thiophene HDS, while the NiMo/(Si/Al)-MCM-41(20) one was the most effective for BPCs HDCl.

References

1. Topsøe H, Clausen BS, Massoth FE (1996) Hydrotreating catalysis. In: Anderson JR, Boudart M (eds) Catalysis—science and technology, vol 11. Springer, Berlin
2. Gary JH, Handwerk GE (1984) Petroleum refining technology and economics. Marcel Dekker Inc., Michigan
3. United States Environmental Protection Agency (2012) Water: CWA methods. Priority pollutants. http://water.epa.gov/scitech/methods/cwa/pollutants.cfm. Retrieved 20 August 2012
4. Buser HR, Bosshardt HP, Rappe C (1978) Chemosphere 7:109
5. Lorenc-Grabowska E, Yperman J, Gryglewicz G, Hoste S, Carleer R (2006) Fuel 85:374
6. la Pierre RB, Guczi L, Kranich WL, Weiss AH (1986) J Catal 52:230
7. Coq B, Ferrat G, Figueras F (1986) J Catal 101:434
8. Creyghton EJ, Burgers MHW, Jansen JC, van Bekkum H (1995) Appl Catal A Gen 128:275
9. Srinivas ST, Lakshmi LJ, Lingaiah N, Sai-Prasad PS, Kanta Rao P (1996) Appl Catal A Gen 135: L201
10. Frimmel J, Zdrazil M (1997) J Catal 167:286
11. Forni P, Prati L, Rossi M (1997) Appl Catal B Environ 14:49
12. Schüth C, Reinhard M (1998) Appl Catal B Environ 18:215
13. Shin EJ, Keane MA (1998) Appl Catal B Environ 18:241
14. Shin EJ, Spiller A, Tavoularis G, Keane MA (1999) Phys Chem Chem Phys 1:3173
15. Lingaiah N, Uddin MA, Muto A, Iwamoto T, Sakata Y, Kusano Y (2000) J Mol Catal A Chem 161:157
16. Keane MA, Murzin DY (2001) Chem Eng Sci 56:3185
17. Hagh B, Allen D (1990) Chem Eng Sci 45:2695
18. Murena F, Famiglietti V, Gioia F (1993) Environ Prog 12:231
19. Murena F, Schioppa E, Gioia F (2000) Environ Sci Technol 34:4382
20. Murena F, Schioppa E (2000) Appl Catal B Environ 27:257
21. Murena F, Gioia F (2002) Appl Catal B Environ 38:39
22. Gryglewicz S, Stolarski M (2003) Pol J Appl Chem 47:23
23. Gioia F, Gallagher EJ, Famiglietti V (1994) J Hazard Mater 38:277
24. Manion JA, Mulder P, Louw R (1985) Environ Sci Technol 19:280
25. Corma A, Kumar D (1998) Actas del XIV SICAT. Cartagena, PL15
26. Song C, Reddy KM (1999) Appl Catal A Gen 176:1
27. de la Paz C, Muñoz A, Burgos E, Rodríguez E (1999) Rev Soc Quím Méx 43:149
28. Kaluza L, Zdrazil M, Zilkova N, Cejka J (2002) Catal Commun 3:151
29. Beck JS, Vartuli JC, Roth WJ, Leonowicz ME, Kresge CT, Schmitt KD, Chu CT-W, Olson DH, Sheppard EW, McCullen SB, Higgins JB, Schlenker JL (1992) J Am Chem Soc 114:10833
30. Silva-Rodrigo R, Hernández-López F, Martínez-Juárez K, Castillo-Mares A, Melo-Banda JA, Olivas-Sarabia A, Ancheyta J, Rana MS (2008) Catal Today 130:309
31. Souza MJB, Marinkovic BA, Jardim PM, Araujo AS, Pedrosa AMG, Souza RR (2007) Appl Catal A Gen 316:212
32. Wang A, Wang Y, Kabe T, Chen Y, Ishihara A, Qian W, Yao P (2002) J Catal 210:319
33. Klimova T, Calderón M, Ramírez J (2003) Appl Catal A Gen 240:29
34. Grzechowiak JR, Mrozinska K, Masalska A, Goóralski J, Rynkowski J, Tylus W (2006) Catal Today 114:272
35. Chiranjeevi T, Kumaran GM, Dhar GM (2008) Petrol Sci Technol 26:690
36. Cesteros Y, Salagre P, Medina F, Sueiras JE (2002) Catal Lett 79:83
37. Selvam P, Mohapatra SK, Sonavane SU, Jayaram RV (2004) Appl Catal B Environ 49:251
38. Kawabata T, Atake I, Ohishi Y, Shishido T, Tian Y, Takaki K, Takehira K (2006) Appl Catal B Environ 66:151
39. López-Gaona A, de los Reyes JA, Aguilar J, Martín N (2010) React Kinet Mech Catal 99:177
40. Power Diffraction File (1995) ICDD. Newtown Square, Philadelphia
41. Laine J, Brito J, Severino F (1985) Appl Catal 15:333
42. American Society for Testing and Materials ASTM (1991) Standard test method for analysis of polychlorinated biphenyls in insulating liquids by gas chromatography, D4059
43. Mokaya R (2002) Enc Phys Sci Tech Inorg Chem 369
44. Zhao XS, Max-Lu GQ, Millar GJ (1996) Ind Eng Chem Res 35:2075
45. Souza MJB, Araújo AS, Pedrosa AMG, Marinkovic BA, Jardim PM, Morgado E (2006) Mater Lett 60:2682
46. Mokaya R, Jones W (1997) J Catal 172:211
47. Melo RAA, Giotto MV, Rocha J, Urquieta-González EA (1999) Mat Res 2:173
48. Liepold A, Roos K, Reschetilowski W, Esculcas AP, Rocha J, Philippou A, Anderson MW (1996) J Chem Soc Faraday Trans 92:4623
49. Luan Z, He H, Zhou W, Cheng C, Klinowski J (1995) J Chem Soc Faraday Trans 91:2955
50. Mokaya R, Jones W, Luan Z, Alba MD, Klinowski J (1996) Catal Lett 37:113
51. Shimada H, Sato T, Yoshimura Y, Hiraishi J, Nishijima A (1988) J Catal 110:275
52. Yue Y, Sun Y, Gao Z (1997) Catal Lett 47:167